

# Altered Diffusion in the Frontal Lobe in Parkinson Disease

A.T. Karagulle Kendi  
S. Lehericy  
M. Luciana  
K. Ugurbil  
P. Tuite

**BACKGROUND AND PURPOSE:** Parkinson disease (PD) is characterized by basal ganglia abnormalities. However, there are neurodegenerative changes in PD that extend beyond the basal ganglia and that are not sufficiently evaluated with standard MR imaging. The aim of this study was to characterize whole-brain gray matter (GM) and white matter (WM) changes in PD by using diffusion tensor imaging (DTI).

**MATERIALS AND METHODS:** Thirteen control and 12 subjects with nondemented PD were examined by using DTI and 3D anatomic T1-weighted images. Statistical parametric mapping analyses of DTI and anatomic images were performed. Patients were evaluated with a variety of neurocognitive measures and the Unified Parkinson's Disease Rating Scale (UPDRS) OFF (cessation of medication) and ON (taking medications as normal) their antiparkinsonian medications.

**RESULTS:** The PD participants had dopa-responsive features as ascertained by the UPDRS OFF versus ON medications and had no cognitive impairment. Decreased fractional anisotropy (FA) was observed in subjects with PD bilaterally in the frontal lobes, including the supplementary motor area, the presupplementary motor area, and the cingulum. There were no significant differences in mean diffusivity or GM/WM attenuation between PD subjects and controls.

**CONCLUSION:** Statistical parametric mapping analysis of DTI showed changes in FA in frontal areas without volume loss. These results confirm that the neurodegenerative process extends beyond the basal ganglia in PD.

Parkinson disease (PD) is a neurodegenerative disorder characterized by bradykinesia, rigidity, resting tremor, and postural abnormalities. In PD, the primary pathologic changes involve loss of nigrostriatal dopaminergic neurons.<sup>1</sup> In addition to dopamine-related motor impairments in PD, there are increasingly recognized nondopaminergic deficits in other brain areas.<sup>1,2</sup> The extension of the neurodegenerative process beyond the basal ganglia is probably the basis for clinical features, including motor and nonmotor, of PD.

For appreciating these pathophysiologic changes in PD, conventional MR imaging has been unsuccessful so far. The development of a noninvasive technology for understanding changes at the microstructural level would be helpful to improve understanding as well as for monitoring disease progression and prognostication regarding these aspects of PD.<sup>3,4</sup> Several authors, summarized in a review article, have stressed the potential utility of recent MR imaging techniques.<sup>4</sup> Voxel-based morphometry assesses whole-brain differences in local gray matter (GM) attenuation by using structural T1-weighted images<sup>5</sup> and provides information on brain atrophy. Voxel-based diffusion tensor imaging (DTI) assesses changes in diffusion orientation and magnitude throughout the whole brain. Voxel-based DTI allows detection of subtle abnormalities in GM and white matter (WM) integrity.<sup>6</sup> In particular,

voxel-based DTI provides information on the orientation of diffusion in WM fiber bundles.

Normal diffusion measurements have been reported in PD in the brain stem, cerebral peduncles, and the basal ganglia, whereas diffusion was altered in patients with multiple system atrophy and progressive supranuclear palsy.<sup>7-12</sup> Few studies have examined whole-brain diffusion imaging in patients with PD. One group found loss of WM integrity in patients with PD compared with healthy subjects in the subcortical WM region containing the nigrostriatal pathway.<sup>13</sup> Another study showed increased apparent diffusion coefficient in the precentral and prefrontal white matter in patients with PD.<sup>11</sup> Last, another group found decreased fractional anisotropy (FA) in the substantia nigra.<sup>14</sup>

On the basis of previous work, we proposed to evaluate whole-brain DTIs of patients with PD and control subjects by using statistical parametric mapping (SPM) analysis (SPM2, Wellcome Department of Cognitive Neurology, Institute of Neurology, London, UK; <http://www.fil.ion.ucl.ac.uk/spm/>) in an attempt to detect GM loss and WM integrity loss.

## Subjects and Methods

### Patients and Controls

Twelve patients with PD (5 men; mean age,  $62.1 \pm 12.7$  years) and 13 age- and sex-matched control subjects (8 men; mean age,  $58.0 \pm 7.3$  years) were included in this University of Minnesota institutional review board–approved study. Patients and controls were recruited by using institutional review board–approved strategies, which included the use of a PD and control subject registry, posted and published advertisements, and approaching potential participants in the clinic. At screening, participants underwent a neurologic history and examination to exclude possible control and PD subjects with potentially confounding neurologic factors or other medical conditions. All

Received June 21, 2007; accepted after revision August 31.

From the Department of Radiology (A.T.K.K., K.U.), Center for Magnetic Resonance Research, University of Minnesota, Minneapolis, Minn; Center for Neuroimaging Research (S.L.), INSERM U610, Pitie-Salpetriere Hospital, University Pierre and Marie Curie, Paris, France; and Departments of Psychology (M.L.) and Neurology (P.T.), University of Minnesota, Minneapolis, Minn.

This work was supported by grants from the Academic Health Center of the University of Minnesota, MN Medical Foundation, and grant M01-RR00400 from the National Center for Research Resources, National Institutes of Health.

Please address correspondence to Paul Tuite, MD, MMC 295, 420 Delaware St SE, Minneapolis, MN 55455; e-mail: [tuite002@umn.edu](mailto:tuite002@umn.edu)

DOI 10.3174/ajnr.A0850

**Table 1: Demographic data and clinical scores of subject population**

Group (No.)	Sex (M/F)	Age (yr)	Disease Duration (yr)	HY	HY	UPDRS	UPDRS	MMSE
		Mean (SD)	Mean (SD)	(ON)	(OFF)	(ON)	(OFF)	(ON)
PD (12)	5/7	62.1 (12.7)	5.8 (4.5)	1.8 (0.4)*	1.9 (0.6)	43 (13.8) <sup>a</sup>	53.3 (22.1)	28.2
Controls (13)	8/5	58.0 (7.3)	N/A	N/A	N/A	N/A	N/A	28.8

**Note:**—NA indicates data not available; M, male; F, female; HY, Hoehn and Yahr clinical staging; UPDRS, Unified Parkinson Disease Rating Scale; MMSE, Mini-Mental State Examination; ON, taking medication as normal; OFF, cessation of medication.  
\* Levodopa equivalent dosage =  $585.2 \pm 509.8$  mg.

enrolled patients with PD were diagnosed as having idiopathic PD according to the Gelb criteria for PD.<sup>15</sup>

### Neurologic Evaluation

Clinical data are presented in Table 1. All patients and controls underwent standardized neurologic testing at their baseline visit by using the Unified Parkinson Disease Rating Scale (UPDRS). Participants with PD did not have dementia as assessed by the Mini-Mental State Examination (MMSE),<sup>16</sup> were taking antiparkinsonian medication, and had a documented clinical response to medication. Disease duration was  $5.8 \pm 4.5$  years. Hoehn and Yahr (HY) clinical staging was  $1.8 \pm 0.4$  ON (taking medications as normal) and  $1.9 \pm 0.6$  OFF (cessation of medication). Total UPDRS scores were  $43.7 \pm 13.8$  ON medication and  $53.3 \pm 22.1$  OFF medication. Patients were treated by using levodopa, ropinirole, or pramipexole alone or in combination. The average daily levodopa equivalent dose was  $585.2 \pm 509.8$  mg.

### Imaging Protocol

All subjects underwent structural MR imaging on a 3T Trio 8-channel MR imaging scanner (Siemens Medical Systems, Erlangen, Germany). All patients were in an ON medication state during MR imaging. The imaging protocol included a coronal 3D T1-weighted sequence of the whole brain with the following parameters: TR, 2530 ms; TE, 3.65 ms; TI, 1100 ms; 1 average; voxel size,  $1 \times 1 \times 1$  mm<sup>3</sup>; matrix size,  $256 \times 192$ ; acquisition time, 487 seconds. The DTIs were acquired by using spin-echo echo-planar images with the following parameters: TR, 7500 ms; TE, 82 ms; flip angle, 90°; matrix,  $128 \times 128$ ; FOV,  $256 \times 256$  mm; section thickness, 2 mm; spacing between sections, 2 mm; number of averages, 3; acquisition time, 339 seconds. Diffusion weighting was performed along 12 independent directions with a b-value of 1000 s/mm<sup>2</sup> and 1 volume acquired without diffusion weighting (b0 image).

### Data Analysis

**SPM Analysis of T1-Weighted Images.** Data processing and analyses were performed by using SPM software (SPM2). Voxel-based morphometry was performed by using an optimized procedure as described in Good et al.<sup>17</sup> The protocol included the following: 1) affine normalization of the T1-weighted image by using a custom study-specific T1 template and the following default parameters: 25-mm cutoff, medium nonlinear regularization, 16 nonlinear iterations; 2) segmentation of GM; 3) estimation of the nonlinear normalization parameters by using the GM template previously built; 4) application of these parameters to the original whole-brain T1-weighted image, which was then resectioned to a voxel size of  $1 \times 1 \times 1$  mm<sup>3</sup>; 5) segmentation of the normalized image into GM by using the customized prior probability map; 6) Jacobian modulation of the segmented GM image; and 7) smoothing of GM images with a 10-mm full width at half maximum isotropic Gaussian kernel. The same process was applied to WM images by using a WM template.

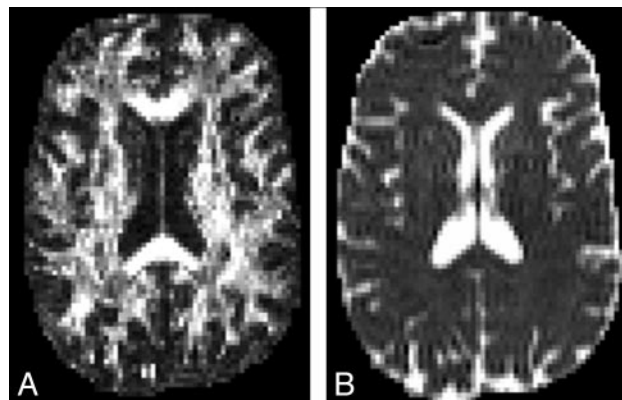


**Fig 1.** Axial FA (A) and MD (B) images of a control subject at the level of the basal ganglia.

**Creation of the Custom Template.** The MR images of all control subjects and patients were used for the creation of the template. Each T1-weighted MR imaging volume was spatially normalized to the T1 Montreal Neurologic Institute (MNI) template with affine registration only. Subsequently, the normalized scans were averaged, and the resulting mean image was smoothed with a 10-mm full width at half maximum Gaussian kernel to form the T1 template. A study-specific GM template was created according to the following steps: spatial normalization of all structural images to the customized T1 template, segmentation into GM partitions, and brain extraction (for removing nonbrain voxels from the GM images). The GM images were averaged to create a GM template respectively and then smoothed with a 10-mm full width at half maximum kernel. A separate WM template was obtained after the following steps: segmentation into WM partition, averaging of WM images to form a WM template, and smoothing with a 10-mm full width at half maximum.

**SPM Analysis of DTIs.** Raw diffusion-weighted data were corrected for geometric distortions secondary to eddy currents by using a registration technique based on the geometric model of distortions.<sup>18</sup> Field map correction was performed by using a double-echo gradient-echo sequence with SPM2 software.

DTI images were first processed to generate FA and mean diffusivity (MD) maps by using in-house software (Fig 1).<sup>19</sup> To allow voxel-based statistical comparisons, we spatially normalized the T2-weighted images obtained for b0 of all subjects by using the MNI template. The FA and MD maps for the whole brain, including the brain stem and cerebellum, were then normalized by using the parameters determined from the normalization of the b0 image. The normalized FA and MD maps were smoothed with a 10-mm isotropic Gaussian kernel.<sup>20</sup>

### Statistical Analysis

Group comparisons for whole-brain T1-weighted images and DTI were performed by using Student *t* tests. Analysis of covariance was performed by using age as a covariable. We used a voxelwise threshold of  $P < .01$  with a corrected  $P < .05$  for cluster extent.

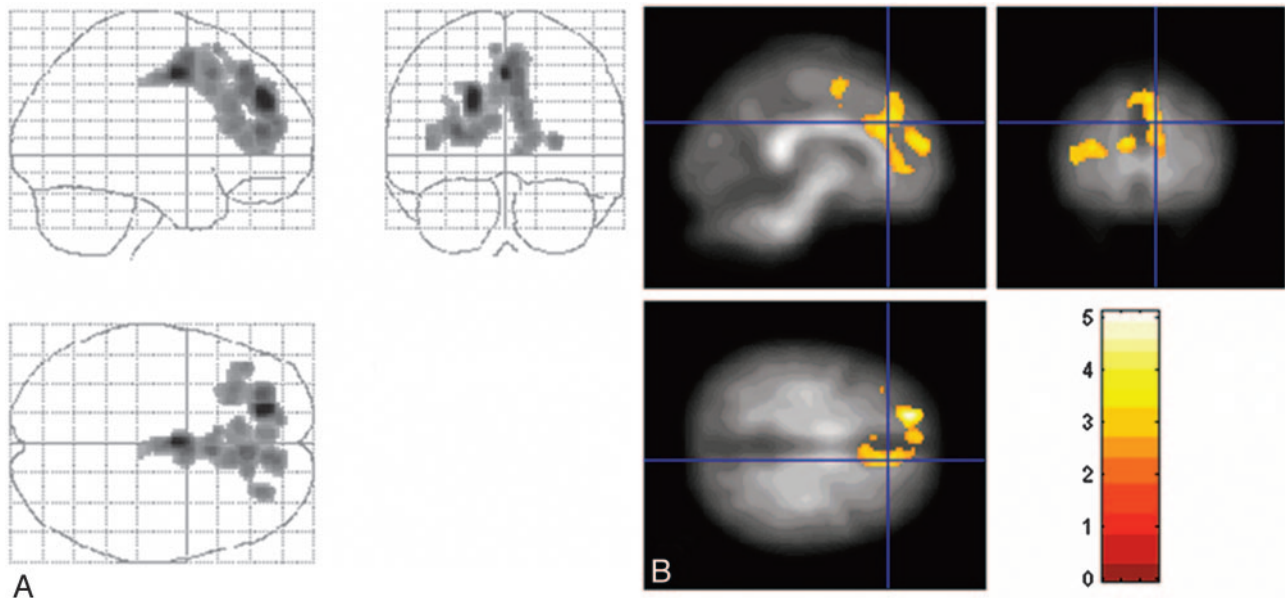


**Fig 2.** *A*, A glass brain showing significant clusters of reduced FA in patients with PD compared with control subjects as viewed from the right (upper left), front (upper right), and above (lower left). SPM display is according to radiologic convention (right-to-left orientation). *B*, The statistical map is superimposed on the normalized average FA image. The images are in MNI space. Color bar indicates z-score. Clusters were considered significant at  $P < .05$ , corrected for multiple comparisons.

## Results

### Demographics

There were no statistically significant differences in age, sex distribution, or MMSE scores between PD and control subjects (Table 1).

### Voxel-Based Morphometry

Comparison of GM and WM volumes of whole brain between PD patients and controls revealed no significant differences.

### Voxel-Based Diffusion Tensor Analysis

**Maps of MD.** There were no significant group differences in MD values.

**Maps of Anisotropy.** Analysis of DTIs of the whole brain, including the brain stem and cerebellum, revealed a significant decrease in FA values in patients with PD bilaterally in the medial frontal cortex, including the supplementary motor area; the pre-supplementary motor area; the right rostral medial frontal gyrus; the left anterior cingulate gyrus; the right and left rostral cingulate gyrus; the right superior, middle, and inferior frontal gyri; and the bilateral middle frontal gyri at the frontal pole. The right superior longitudinal fasciculus and left corpus callosum were also involved within the significant cluster (Fig 2 and Table 2). There were no areas with significantly increased FA. A difference in z-scores and volume of significant voxels was noted between hemispheres, which was primarily due to involvement in the dorsolateral prefrontal cortex and medial frontal lobes. The cluster was larger and z-scores were higher in the left hemisphere. However, the SPM analysis does not directly compare the 2 hemispheres.

### Discussion

This study shows a significant decrease in FA values in the frontal lobes, including supplementary motor area, prefrontal areas, and the anterior cingulate area in patients with PD com-

pared with age-matched controls. Diffusion abnormalities were not associated with GM or WM changes because voxel-based morphometry comparison did not show any difference between patients and control subjects.

DTI, a recently developed MR imaging technique, provides more subtle information about WM integrity. It is a unique form of imaging enabling us to quantify the thermal random motion of water molecules.<sup>6,21</sup> Within the brain, the coherent orientation of axons constrains water molecules to move preferentially along the main direction of neural fibers, a property called anisotropy. Anisotropy can be considered a measurable parameter of organization of axons. Anisotropy has been used to identify fiber tracts. The FA value is derived from eigenvalues of the diffusion tensor and is a measure of the anisotropy of water diffusion in tissue. Lower FA means decrease in fiber coherence of the connecting tract.

Normal diffusion measurements have been reported in several studies by using regions of interest in PD. Diffusion was normal in the brain stem, cerebral peduncles, and the basal ganglia; whereas it was altered in multiple-system atrophy and in patients with progressive supranuclear palsy.<sup>7-12</sup> In a recent DTI study by Yoshikawa et al,<sup>13</sup> decreased FA was reported in an area containing the nigrostriatal fibers in patients with PD, suggesting that FA decreases could parallel other neuronal changes in the brain.<sup>13</sup> Recently Chan et al<sup>14</sup> demonstrated, in a large prospective case-control study, that FA values in the substantia nigra were lower in patients with PD compared with healthy controls and correlated inversely with the clinical severity of PD.<sup>14</sup>

We did not reproduce the findings of either group. The failure to replicate their results could be due to the smaller number of subjects enrolled in our study versus the large number studied in the work by Chan et al,<sup>14</sup> differences in the severity of disease, or possibly related to imaging techniques and postprocessing methods. Yoshikawa et al<sup>13</sup> did a region-

**Table 2: Peaks for significant clusters of decreased FA in patients with PD\***

PD Versus Controls	Hemisphere	Brodmann Area	MNI Coordinates			Z-Score
			x	y	z	
Medial frontal cortex						
SMA	L	6	-4	14	46	3.3
Pre-SMA	R	8	4	26	52	2.79
	R	6	6	18	60	2.83
Rostral medial frontal gyrus	R	9	6	46	36	2.97
Cingulate cortex						
Anterior cingulate gyrus		24	0	-6	46	4.12
	L	24	-6	34	46	3.41
		32	0	14	38	3.00
	L	32	-8	26	28	3.11
Rostral cingulate gyrus	R	24	10	30	18	3.00
	L	32	-8	44	2	2.82
	L	9	-8	46	22	3.18
Dorsolateral prefrontal cortex						
Superior frontal gyrus	R	9	18	44	32	4.14
Middle frontal gyrus	R	46	28	42	14	3.50
Inferior frontal gyrus	R	46	42	34	6	2.93
Frontal pole						
Middle frontal gyrus	R	10	20	46	10	3.17
	L	10	-28	42	8	3.06
WM bundles						
Superior longitudinal fasciculus	R		30	26	16	3.09
Corpus callosum	L		-16	34	10	3.02

**Note:**—SMA indicates supplementary motor area; MNI, Montreal Neurologic Institute.  
\* All significant maxima were part of a single large cluster, including 3927 voxels.

of-interest analysis for subcortical nuclei, including the subcortical WM of the prefrontal cortex (area 6), the head of the caudate, the putamen, and the substantia nigra. In the current study, whole-brain analysis was performed; therefore, it may not detect subtle changes that can be appreciated with region-of-interest analysis. We opted not to use region-of-interest analysis because this method seems limited compared with voxel-based DTI to evaluate the entire brain. Recently, Snook et al<sup>22</sup> suggested that voxel-based DTI and region-of-interest techniques are complementary but still unable to completely reflect ongoing changes.<sup>22</sup> They also offered tractography as a potentially better alternative to 2D region-of-interest and voxel-based analysis.

The presence of diffusion changes in the frontal lobes in patients with PD compared with controls may have several explanations. First, the diffusion abnormalities may be associated with the pathologic process in PD. The finding of decreased FA values in the frontal WM in patients with PD, and particularly the supplementary motor area and cingulate cortex, is in line with evidence that neurodegenerative changes may occur outside the substantia nigra.<sup>2</sup>

Second, diffusion changes may be reflective of frontal lobe dysfunction in PD. Functional neuroimaging studies have repeatedly shown changes in activation in motor and premotor areas in PD during performance of motor tasks, particularly in the supplementary motor area.<sup>23-29</sup> Dysfunction of medial frontal areas, which presumably results from altered basal ganglia interactions due to nigrostriatal dopaminergic loss, plays a role in impaired motor performance (ie, hypokinesia).<sup>1,30</sup> This type of functional cortical deafferentation is supported by brain imaging studies showing diminished regional blood flow in the supplementary motor area<sup>24</sup> and the prefrontal region.<sup>23</sup>

Morphologic longitudinal imaging studies have shown significant annual brain volume loss in patients with PD without dementia compared with control subjects.<sup>31</sup> Frontal lobe atrophy, which correlates with the duration of motor symptoms, has been described in the late-onset PD,<sup>32</sup> and frontal lobe changes were found in patients with PD with early cognitive impairment and those with dementia,<sup>33-35</sup> as well as patients without dementia.<sup>34,36,37</sup> Our results complement these studies in showing that diffusion abnormalities can occur in the frontal lobe in patients with PD. However, we did not find brain atrophy, even in the frontal or temporal cortices, as suggested by the lack of significant GM and WM volume differences between patients with PD and controls.

One possible explanation for the failure to replicate the finding of atrophy may be the small sample size in this study. Second, the lack of confirmatory pathology limits interpretation of this as well as the work of others. Clearly, it would be helpful to know that all participants with a clinical diagnosis of PD actually have PD pathology, in addition to having similar severity of changes and the distribution of involvement outside the substantia nigra. Additionally, the presence of accompanying neuropathology (eg, vascular and/or Alzheimer changes) may also be a potential confound, though the high MMSE scores demonstrated by these participants argue against the presence of concomitant dementia. These types of changes, if present, would be subtle.

Meanwhile voxel-based morphometry analysis has its own limitations. Spatial normalization is used to map each image to a template. Recent use of customized T1 templates rather than a standard template has been implemented to reduce potential errors that may limit regional specificity.<sup>34</sup> In our study, we also used a custom template to reduce errors. Given the older age of this study population, it is possible that with

aging, reduced tissue contrast may limit differentiation of the voxels, resulting in misclassification during segmentation.<sup>34</sup> So atrophic changes reported in deep brain nuclei in other studies may need further validation due to the fact that these areas are prone to artifacts from segmentation.

## Conclusion

DTI revealed diffusion changes in frontal areas in patients with PD compared with control subjects. These results suggest that neurodegenerative changes may occur outside the substantia nigra in PD.

## Acknowledgments

We thank patients and control subjects who participated in this study as well as Stacy Majestic and Kim Krawczewski, who helped with coordination.

## References

1. Obeso JA, Rodriguez-Oroz MC, Rodriguez M, et al. Pathophysiology of the basal ganglia in Parkinson's disease. *Trends Neurosci* 2000;23:S8–19
2. Braak H, Braak E. Pathoanatomy of Parkinson's disease. *J Neurol* 2000; 247(suppl 2):II3–10
3. Tambasco N, Pelliccioli GP, Chiarini P, et al. Magnetization transfer changes of grey and white matter in Parkinson's disease. *Neuroradiology* 2003;45:224–30
4. Seppi K, Schocke MF. An update on conventional and advanced magnetic resonance imaging techniques in the differential diagnosis of neurodegenerative parkinsonism. *Curr Opin Neurol* 2005;18:370–75
5. Ashburner J, Friston KJ. Voxel-based morphometry: the methods. *Neuroimage* 2000;11:805–21
6. Le Bihan D, Mangin JF, Poupon C, et al. Diffusion tensor imaging: concepts and applications. *J Magn Reson Imaging* 2001;13:534–46
7. Schocke MF, Seppi K, Esterhammer R, et al. Diffusion-weighted MRI differentiates the Parkinson variant of multiple system atrophy from PD. *Neurology* 2002;58:575–80
8. Seppi K, Schocke MF, Esterhammer R, et al. Diffusion-weighted imaging discriminates progressive supranuclear palsy from PD, but not from the parkinson variant of multiple system atrophy. *Neurology* 2003;60:922–27
9. Schocke MF, Seppi K, Esterhammer R, et al. Trace of diffusion tensor differentiates the Parkinson variant of multiple system atrophy and Parkinson's disease. *Neuroimage* 2004;21:1443–51
10. Blain CR, Barker GJ, Jarosz JM, et al. Measuring brain stem and cerebellar damage in parkinsonian syndromes using diffusion tensor MRI. *Neurology* 2006;67:2199–205
11. Nicoletti G, Lodi R, Condino F, et al. Apparent diffusion coefficient measurements of the middle cerebellar peduncle differentiate the Parkinson variant of MSA from Parkinson's disease and progressive supranuclear palsy. *Brain* 2006;129:2679–87
12. Paviour DC, Thornton JS, Lees AJ, et al. Diffusion-weighted magnetic resonance imaging differentiates Parkinsonian variant of multiple-system atrophy from progressive supranuclear palsy. *Mov Disord* 2007;22:68–74
13. Yoshikawa K, Nakata Y, Yamada K, et al. Early pathological changes in the parkinsonian brain demonstrated by diffusion tensor MRI. *J Neurol Neurosurg Psychiatry* 2004;75:481–84
14. Chan LL, Rumpel H, Yap K, et al. Case-control study of diffusion tensor imaging in Parkinson's disease. *J Neurol Neurosurg Psychiatry* 2007;78:1383–86. Epub 2007 Jul 5
15. Gelb DJ, Oliver E, Gilman S. Diagnostic criteria for Parkinson disease. *Arch Neurol* 1999;56:33–39
16. Folstein MF, Folstein SE, McHugh PR. "Mini-mental state": a practical method for grading the cognitive state of patients for the clinician. *J Psychiatr Res* 1975;12:189–98
17. Good CD, Johnsrude IS, Ashburner J, et al. A voxel-based morphometric study of ageing in 465 normal adult human brains. *Neuroimage* 2001;14:21–36
18. Mangin JF, Poupon C, Clark C, et al. Distortion correction and robust tensor estimation for MR diffusion imaging. *Med Image Anal* 2002;6:191–98
19. Lehericy S, Ducros M, Krainik A, et al. 3-D diffusion tensor axonal tracking shows distinct SMA and pre-SMA projections to the human striatum. *Cerebral Cortex* 2004;14:1302–09. Epub 2004 May 27
20. Thivard L, Lehericy S, Krainik A, et al. Diffusion tensor imaging in medial temporal lobe epilepsy with hippocampal sclerosis. *Neuroimage* 2005;28:682–90
21. Scherfler C, Schocke MF, Seppi K, et al. Voxel-wise analysis of diffusion weighted imaging reveals disruption of the olfactory tract in Parkinson's disease. *Brain* 2006;129(Pt 5):538–42. Epub 2005 Nov 4
22. Snook L, Plewes C, Beaulieu C. Voxel based versus region of interest analysis in diffusion tensor imaging of neurodevelopment. *Neuroimage* 2007;34:243–52. Epub 2006 Oct 27
23. Playford ED, Jenkins IH, Passingham RE, et al. Impaired mesial frontal and putamen activation in Parkinson's disease: a positron emission tomography study. *Ann Neurol* 1992;32:151–61
24. Samuel M, Ceballos-Baumann AO, Blin J, et al. Evidence for lateral premotor and parietal overactivity in Parkinson's disease during sequential and bimanual movements: a PET study. *Brain* 1997;120(Pt 6):963–76
25. Catalan MJ, Ishii K, Honda M, et al. A PET study of sequential finger movements of varying length in patients with Parkinson's disease. *Brain* 1999; 122(Pt 3):483–95
26. Sabatini U, Boulanouar K, Fabre N, et al. Cortical motor reorganization in akinetic patients with Parkinson's disease: a functional MRI study. *Brain* 2000;123(Pt 2):394–403
27. Haslinger B, Erhard P, Kampfe N, et al. Event-related functional magnetic resonance imaging in Parkinson's disease before and after levodopa. *Brain* 2001;124:558–70
28. Mentis MJ, Dhawan V, Nakamura T, et al. Enhancement of brain activation during trial-and-error sequence learning in early PD. *Neurology* 2003;60:612–19
29. Turner RS, Grafton ST, McIntosh AR, et al. The functional anatomy of parkinsonian bradykinesia. *Neuroimage* 2003;19:163–79
30. Kikuchi A, Takeda A, Kimpara T, et al. Hypoperfusion in the supplementary motor area, dorsolateral prefrontal cortex and insular cortex in Parkinson's disease. *J Neurol Sci* 2001;193:29–36
31. Hu MT, White SJ, Chaudhuri KR, et al. Correlating rates of cerebral atrophy in Parkinson's disease with measures of cognitive decline. *J Neural Transm* 2001;108:571–80
32. Double KL, Halliday GM, McRitchie DA, et al. Regional brain atrophy in idiopathic Parkinson's disease and diffuse Lewy body disease. *Dementia* 1996;7:304–13
33. Owen AM, Doyon J. The cognitive neuropsychology of Parkinson's disease: a functional neuroimaging perspective. *Adv Neurol* 1999;80:49–56
34. Burton EJ, McKeith IG, Burn DJ, et al. Cerebral atrophy in Parkinson's disease with and without dementia: a comparison with Alzheimer's disease, dementia with Lewy bodies and controls. *Brain* 2004;127:791–800
35. Beyer MK, Janvin CC, Larsen JP, et al. A magnetic resonance imaging study of patients with Parkinson's disease with mild cognitive impairment and dementia using voxel-based morphometry. *J Neurol Neurosurg Psychiatry* 2007;78:254–59
36. Nagano-Saito A, Washimi Y, Arahata Y, et al. Cerebral atrophy and its relation to cognitive impairment in Parkinson disease. *Neurology* 2005;64:224–29
37. Summerfield C, Junque C, Tolosa E, et al. Structural brain changes in Parkinson disease with dementia: a voxel-based morphometry study. *Arch Neurol* 2005;62:281–85